

The DExD/H box ATPase Dhh1 functions in translational repression, mRNA decay, and processing body dynamics

Johanna S. Carroll, Sarah E. Munchel, and Karsten Weis

Department of Molecular and Cell Biology, Division of Cell and Developmental Biology, University of California, Berkeley, Berkeley, CA 94720

Translation, storage, and degradation of messenger ribonucleic acids (mRNAs) are key steps in the post-transcriptional control of gene expression, but how mRNAs transit between these processes remains poorly understood. In this paper, we functionally characterized the DExD/H box adenosine triphosphatase (ATPase) Dhh1, a critical regulator of the cytoplasmic fate of mRNAs. Using mRNA tethering experiments in yeast, we showed that Dhh1 was sufficient to move an mRNA from an active state to translational repression. In actively dividing cells,

translational repression was followed by mRNA decay; however, deleting components of the 5'–3' decay pathway uncoupled these processes. Whereas Dhh1's ATPase activity was not required to induce translational inhibition and mRNA decay when directly tethered to an mRNA, ATP hydrolysis regulated processing body dynamics and the release of Dhh1 from these RNA–protein granules. Our results place Dhh1 at the interface of translation and decay controlling whether an mRNA is translated, stored, or decayed.

Introduction

Central to the proper regulation of gene expression is the post-transcriptional control of mRNA translation, storage, and decay. By repressing translation and promoting mRNA decay, cells are able to rapidly alter the transcripts that are available for protein production and to attenuate gene expression accordingly.

In eukaryotes, mRNA is stabilized by a 5' methylguanosine cap and a 3' poly(A) tail. The cap-binding protein eIF4E and poly(A)-binding protein interact with the mature transcript, preventing its degradation and promoting its association with translation initiation factors (Coller and Parker, 2004; Garneau et al., 2007). The bulk of eukaryotic mRNA turnover initiates with deadenylation (Coller and Parker, 2004). Shortening of the poly(A) tail is the only reversible step in mRNA turnover; transcripts can be readenylated and return to polysomes to be actively translated (Curtis et al., 1995; Coller and Parker, 2004). However, if an RNA is destined for decay, deadenylation is followed by mRNA degradation. Degradation occurs through one of two conserved pathways: either the unprotected 3' end is degraded by the exosome, a complex of 3'–5' exonucleases,

or, alternatively, and more commonly in yeast, the Dcp1/Dcp2 decapping enzyme cleaves the 5' cap structure, exposing the mRNA to the 5'–3' exonuclease Xrn1 (Coller and Parker, 2004; Garneau et al., 2007). Decapping is a key step in mRNA decay, as the presence of the cap is critical for translation of many transcripts, and its removal activates decay. The decapping machinery and the translation initiation machinery are thought to compete to determine the fate of an mRNA, and initial steps triggering RNA decay involve shortening the poly(A) tail and removing translation factors from a messenger RNP (mRNP) complex (Franks and Lykke-Andersen, 2008).

Nontranslating mRNPs localize in distinct mRNP granules in the cytoplasm (Anderson and Kedersha, 2006; Parker and Sheth, 2007). One class of these mRNP granules, termed processing bodies (PBs), are evolutionarily conserved structures that contain nontranslating mRNAs and proteins involved in decapping, exonucleolytic decay, nonsense-mediated decay (NMD), and microRNA (miRNA)-mediated repression (Eulalio et al., 2007; Parker and Sheth, 2007). The mechanisms involved in the movement of mRNA from polysomes into PBs are unclear;

Correspondence to Karsten Weis: kweis@berkeley.edu

S.E. Munchel's present address is Prognosys Biosciences, La Jolla, CA 92037.

Abbreviations used in this paper: CBP, CaM-binding peptide; miRNA, microRNA; mRNP, messenger RNP; NMD, nonsense-mediated decay; PB, processing body; PP7CP, PP7 coat protein; SSC, saline-sodium citrate; TEV, tobacco etch virus; UTR, untranslated region.

© 2011 Carroll et al. This article is distributed under the terms of an Attribution–Noncommercial–Share Alike–No Mirror Sites license for the first six months after the publication date [see <http://www.rupress.org/terms>]. After six months it is available under a Creative Commons License [Attribution–Noncommercial–Share Alike 3.0 Unported license, as described at <http://creativecommons.org/licenses/by-nc-sa/3.0/>].

however, it is assumed that changes in the protein composition of the mRNP are critical for this relocalization.

Likely candidates for remodeling protein–RNA complexes are members of the DExD/H box family of ATPases. DExD/H box proteins have RNA-dependent ATPase activity and have been shown to have a wide array of activities, including the ability to separate duplex RNA, dissociate proteins bound to RNA (RNPase activity), or function as RNA-binding scaffolds onto which cofactors bind (Rocak and Linder, 2004; Cordin et al., 2006).

The *Saccharomyces cerevisiae* protein Dhh1 is a DExD/H box protein involved in both translational repression and mRNA decay, making it a good candidate for mediating the mRNP remodeling required to move an mRNA from active translation to a translationally inactive state. Dhh1 is part of a highly conserved subfamily of proteins, which includes orthologues in *Schizosaccharomyces pombe* (Ste13), *Caenorhabditis elegans* (CGH-1), *Xenopus laevis* (Xp54), *Drosophila melanogaster* (Me31b), and mammals (RCK/p54). Overexpression of RCK/p54, Xp54, or Me31b can rescue the loss of Dhh1 in yeast (Maekawa et al., 1994; Tseng-Rogenski et al., 2003; Westmoreland et al., 2003), suggesting that the function of this protein is conserved across eukaryotes. Dhh1 and its orthologues interact with proteins essential for decapping, deadenylation, and translational repression (Coller et al., 2001; Fischer and Weis, 2002; Maillet and Collart, 2002; Weston and Sommerville, 2006) and localize to PBs under conditions of cellular stress (Sheth and Parker, 2003; Coller and Parker, 2005; Teixeira et al., 2005). Functionally, Dhh1 is thought to act as an enhancer of decapping because deletion of Dhh1 in yeast stabilizes mRNA transcripts and inhibits decapping (Coller et al., 2001; Fischer and Weis, 2002). In addition to its involvement in decay, Dhh1 and its orthologues have been implicated in both general and miRNA-mediated translational repression (Nakamura et al., 2001; Navarro et al., 2001; Minshall and Standart, 2004; Coller and Parker, 2005; Chu and Rana, 2006; Minshall et al., 2009). For example, recombinant Dhh1 can repress translation of a reporter mRNA in vitro (Coller and Parker, 2005), and both Xp54 and Me31b can repress translation of a reporter mRNA in *Xenopus* oocytes and *Drosophila* S2 cells, respectively (Minshall and Standart, 2004; Minshall et al., 2009; Tritschler et al., 2009). Additionally, Xp54, Me31b, and CGH1 are all components of stored maternal RNPs and are involved in amassing these RNAs in a translationally repressed state (Minshall et al., 2001; Nakamura et al., 2001; Navarro et al., 2001; Minshall and Standart, 2004; Coller and Parker, 2005).

Together, these observations suggest that Dhh1 plays an important role in regulating the translation status of mRNA. However, the mechanism by which Dhh1 directs the fate of an mRNA remains unclear. Here, we investigate the role of Dhh1 in translational repression and decay by tethering Dhh1 to endogenous mRNAs and by analyzing the in vivo role of ATP hydrolysis by Dhh1 in *S. cerevisiae*. We found that tethering Dhh1 reduces both steady-state mRNA and protein and that the reduction in mRNA, but not protein, depends on the 5'–3' decay machinery. ATP hydrolysis is not required for the ability of Dhh1 to reduce mRNA and protein levels when tethered to an mRNA

but is critical for the movement of Dhh1 out of PBs. Our data demonstrate that Dhh1 acts as a translational repressor and decay activator in vivo and support a model in which Dhh1 regulates the transition of an mRNA between active translation, translational repression, and decay.

Results and discussion

Steady-state RNA and protein levels decrease upon tethering Dhh1 to endogenous yeast mRNAs

To dissect the role of Dhh1 in mRNA decay and translational repression, we directly tethered Dhh1 to endogenous mRNAs in vivo by expressing a Dhh1 PP7 coat protein (PP7CP) fusion in a yeast strain containing a target mRNA with a stem–loop binding site for the PP7CP in its 3' untranslated region (UTR; Fig. 1 A). Dhh1-PP7CP rescued the growth defect of a *dhh1Δ* strain, demonstrating that the fusion protein is functional (unpublished data).

We first tethered Dhh1 to an mRNA coding for *fructose 1,6-bisphosphate aldolase (FBA1)*. *FBA1* is essential and is among the most highly expressed mRNAs in yeast (Holstege et al., 1998). Insertion of the PP7 loop into the 3' UTR of *FBA1* did not cause any growth defects, indicating that the loop itself did not interfere with the expression of *FBA1*. To monitor the effects of Dhh1 tethering on *FBA1*, we analyzed steady-state RNA levels by Northern blotting when Dhh1-PP7CP, GFP-PP7CP, or nontethered Dhh1-GFP was present (Fig. 1 B, left). Tethering Dhh1 to *FBA1* mRNA resulted in a fourfold reduction in mRNA levels (Fig. 1 B, left), whereas tethering GFP had no effect on the *FBA1* mRNA levels compared with the no tether control with both Dhh1-PP7CP and GFP-PP7CP expressed at similar levels (Figs. 1 B and S1 A). The reduction in *FBA1* mRNA by Dhh1-PP7CP was dependent on the presence of a PP7-binding loop in the 3' UTR of *FBA1* (Fig. S1 D).

Next, we compared Fba1 protein levels in cells expressing Dhh1-GFP, GFP-PP7CP, or Dhh1-PP7CP (Fig. 1 B, right). Tethering Dhh1 to *FBA1* mRNA resulted in an approximately fourfold reduction in Fba1 protein levels (Fig. 1 B, right). This reduction was again specific to Dhh1-PP7CP and was dependent on the presence of a PP7-binding loop in the 3' UTR of *FBA1* (Figs. 1 B and S1 E).

To test whether Dhh1 could reduce steady-state mRNA and protein levels of other mRNAs, we tethered Dhh1 to *RPL25* mRNA, which encodes an essential ribosomal protein. As for *FBA1*, tethering Dhh1 to *RPL25* mRNA resulted in a fourfold reduction in both protein and mRNA levels when compared with GFP-PP7CP and the nontethered Dhh1-GFP control (Fig. 1 C). Together, these results demonstrate that binding of Dhh1 to yeast mRNAs is sufficient to reduce both steady-state mRNA and protein levels.

The ability of Dhh1 to reduce mRNA levels depends on components of the 5'–3' decay pathway

Next, we wanted to determine whether Dhh1 requires the 5'–3' decay machinery to lower mRNA levels and whether the reduction in protein levels is merely a consequence of the lower

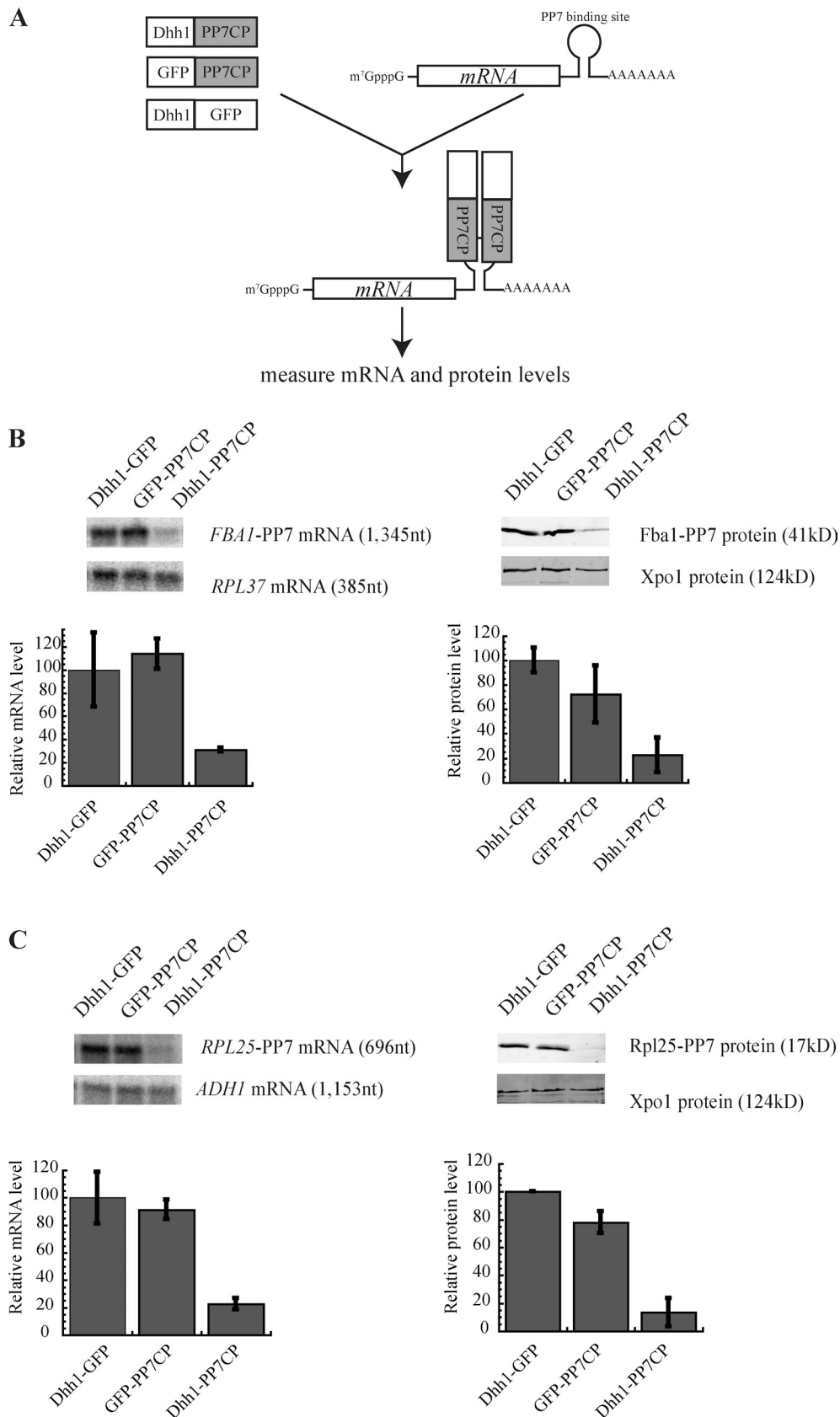


Figure 1. **Tethering Dhh1 to endogenous mRNAs decreases mRNA and protein levels.** (A) A schematic of tethering strategy. (B, left) Northern blot analysis of *FBA1*-PP7 mRNA levels in cells expressing the nontethered control (Dhh1-GFP), GFP-PP7CP, or Dhh1-PP7CP proteins. *FBA1* mRNA levels were normalized to *RPL37* mRNA. (right) Western blot analysis of Fba1 protein levels relative to Xpo1. (C, left) Northern blot analysis of *RPL25*-PP7 mRNA in cells expressing Dhh1-GFP, GFP-PP7CP, or Dhh1-PP7CP proteins normalized to *ADHI* mRNA. (right) Western blot analysis of Rpl25 protein levels normalized to Xpo1. (B and C) Mean values \pm SD from three independent experiments are shown.

mRNA levels or whether Dhh1 directly represses translation. To analyze the role of the 5′–3′ decay pathway, we deleted *CCR4*, a component of the deadenylation complex (Tucker et al., 2001). *FBA1*-PP7 mRNA in *ccr4Δ* yeast remained decreased (about threefold) upon Dhh1 tethering (Fig. 2 A, left). This suggests that recruitment of Dhh1 bypasses the need for deadenylation, consistent with prior results showing that Dhh1 functions downstream of deadenylation (Coller et al., 2001; Fischer and Weis, 2002). In contrast, deletion of the decapping factor *DCP1* (Fig. 2 A, middle) or the 5′–3′ exonuclease *XRN1* (Fig. 2 A, right) restored *FBA1*-PP7 mRNA to normal levels. Thus, the ability of Dhh1 to reduce mRNA levels depends on *DCP1* and *XRN1*, indicating that Dhh1 functions upstream of decapping and exonucleolytic digestion by activating and/or recruiting the 5′–3′ decay machinery.

Dhh1 can reduce protein levels in the absence of RNA decay

The ability to uncouple the tethering of Dhh1 from the subsequent induction of mRNA degradation in *dcp1Δ* and *xrn1Δ* cells allowed us to determine the effects of Dhh1 on protein levels independent of mRNA decay. We compared Fba1 protein levels in *ccr4Δ*, *dcp1Δ*, and *xrn1Δ* strains when Dhh1 was tethered to *FBA1* mRNA. As expected, tethering of Dhh1 to *FBA1* mRNA in the *ccr4Δ* strain resulted in a decrease in Fba1 protein levels, corresponding to the decrease in mRNA levels (Fig. 2, A and B, left). Intriguingly, we found that tethering Dhh1 to *FBA1* mRNA in both the *dcp1Δ* and *xrn1Δ* strains still resulted in a decrease in Fba1 protein levels (Fig. 2 B, middle and right), despite the fact that there was no change in *FBA1* mRNA levels (Fig. 2 A). This shows that Dhh1 can repress mRNA translation independent of its ability to activate mRNA decay and indicates that translational inhibition functions upstream of mRNA decay. If the pathways of mRNA decay and translational inhibition acted in parallel and were in competition with each other, restoration of mRNA levels should at least partially restore steady-state protein levels. However, the Dhh1-mediated decrease in protein levels is identical in wild-type cells and mutants in which the 5′–3′ RNA decay pathway is blocked (compare Fig. 1 with Fig. 2), suggesting that Dhh1-mediated mRNA decay is epistatic to translational repression.

Our data also show that in actively growing yeast, recruitment of Dhh1 to an mRNA rapidly targets the mRNA for decay. It is likely, however, that in different cellular environments or growth conditions, Dhh1's association with an mRNA could result in storage rather than decay. This could be achieved either through recruitment of additional cofactors or through general inhibition of the mRNA decay machinery. In this context, it is interesting that two Dhh1-interacting proteins in yeast have recently been shown to modulate mRNA storage and decay specifically during G_0 (Talarek et al., 2010), and the orthologue of Dhh1 in *C. elegans* is found in distinct complexes depending on the developmental status of the organism (Boag et al., 2008). Additionally, tethering the Dhh1 orthologue to an mRNA in *Xenopus* oocytes, cells with very low decapping activity (Gillian-Daniel et al., 1998), resulted exclusively in translational repression (Minshall and Standart, 2004; Minshall et al., 2009).

Tethering Dhh1 is sufficient to localize *FBA1* mRNA to PBs

In yeast, the mRNA decay machinery localizes to cytoplasmic PBs during certain conditions of cell stress (Parker and Sheth, 2007), and it has been suggested that the number and size of PBs correlate with the amount of nontranslating mRNA (Franks and Lykke-Andersen, 2008). Because tethering Dhh1 to *FBA1* mRNA results in translational repression and mRNA decay, we wanted to test whether tethering Dhh1 to *FBA1* mRNA affects PB formation. To visualize PBs, we expressed Dcp2-GFP in *dhh1Δ* cells with either Dhh1-PP7CP or PP7CP and *FBA1* or *FBA1* containing the PP7-binding loop (Fig. 3 A). Few Dcp2-positive PBs could be detected in cells expressing the PP7CP in either the presence or absence of the PP7-binding loop in the *FBA1* mRNA. Expression of Dhh1-PP7CP alone caused an increase in Dcp2-positive PB intensity compared with PP7CP. Importantly, however, tethering Dhh1 to *FBA1* mRNA resulted in a twofold increase in the amount of Dcp2-GFP found in PBs compared with the nontethered control (Fig. 3 A), demonstrating that tethering Dhh1 to an abundant mRNA can result in increased PB formation.

Next, we tested whether Dhh1 tethering to *FBA1* mRNA was sufficient to localize *FBA1* mRNA to PBs. However, we were unable to detect any enrichment of *FBA1* mRNA in Dcp2-GFP-labeled PBs in a wild-type strain background (unpublished data). Because Dhh1 tethering leads to a drastic reduction of steady-state *FBA1* mRNA levels (Fig. 1), we reasoned that *FBA1* mRNA turnover might be too rapid to observe PB accumulation or, alternatively, that *FBA1* mRNA levels are potentially too low to be visualized by in situ hybridization. Therefore, we monitored the localization of *FBA1* mRNA in *xrn1Δ* cells. In this background, *FBA1*-PP7 mRNA levels are restored, but tethering Dhh1 to *FBA1* still results in translational repression (Fig. 2). Whereas deleting *XRN1* caused the constitutive formation of Dcp2-containing PBs (Fig. 3 B; Teixeira and Parker, 2007), we found that *FBA1* mRNA tethered to the PP7CP alone was enriched in only ~5% of the Dcp2-labeled PBs (Fig. 3 B). In contrast, tethering Dhh1-PP7CP to *FBA1* mRNA resulted in a fivefold increase in the number of PBs in which a signal for *FBA1* mRNA was detected (Fig. 3 B). Targeting of *FBA1* mRNA to PBs required the recruitment of Dhh1, as there was no change in the localization of *FBA1* mRNA that lacked the PP7-binding loop (Fig. 3 B). This demonstrates that tethering Dhh1 to *FBA1* mRNA under conditions in which it causes translational repression results in an increased localization of *FBA1* mRNA to Dcp2-positive PBs. Thus, our results show that recruitment of Dhh1 to a specific mRNA is sufficient to target the resulting mRNP to a PB.

Reduction in RNA and protein levels does not require ATP hydrolysis by Dhh1

Dhh1 is a member of the large family of DEXD/H box ATPases. To investigate the role of Dhh1's ATPase activity in translational inactivation, degradation, and PB localization, we mutated the glutamic acid (E) to glutamine (Q) in the DEAD domain (hereafter referred to as DQAD) of Dhh1. This mutation abolishes ATP hydrolysis activity in several DEXD/H box proteins and is

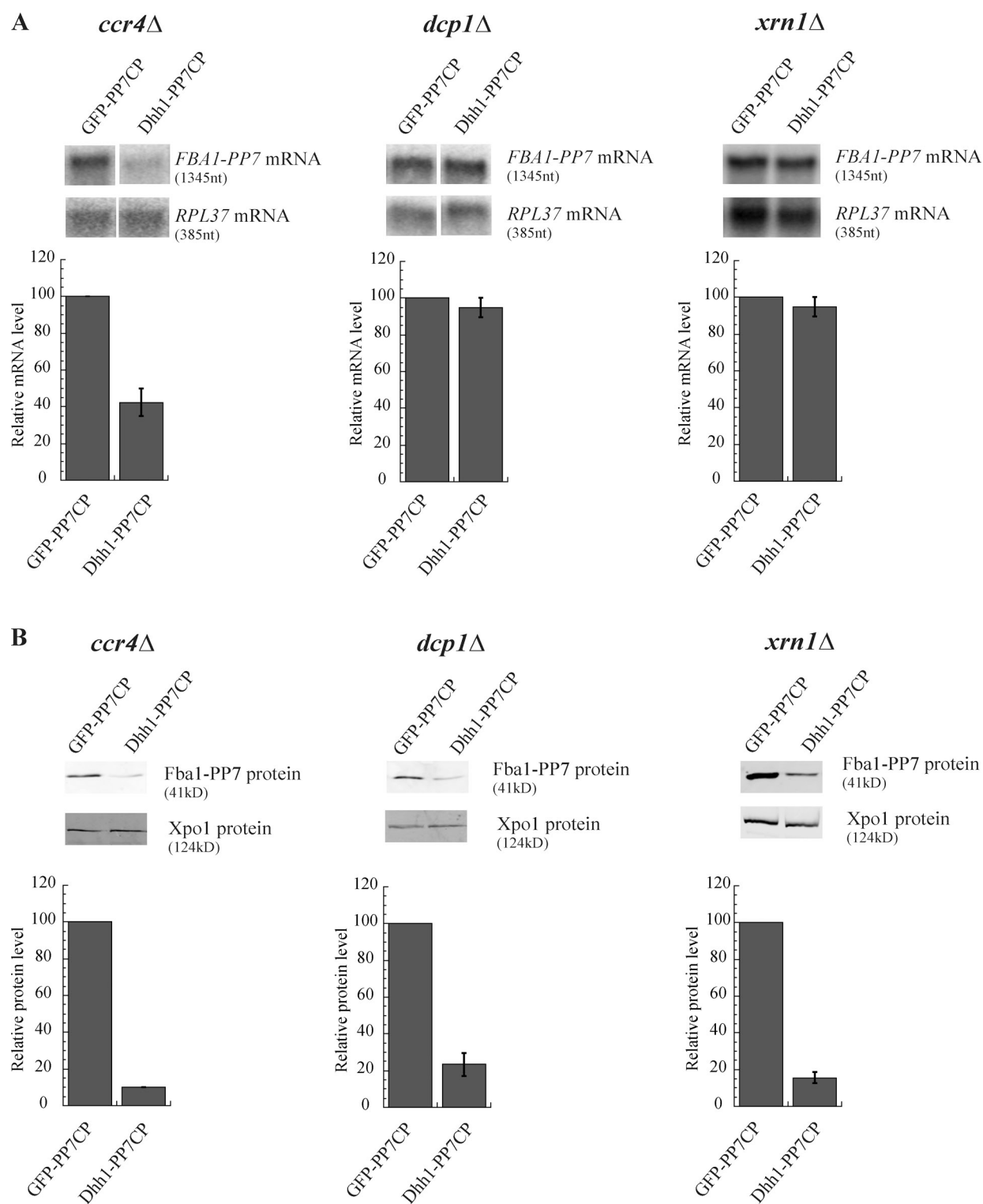


Figure 2. Dhh1's ability to reduce mRNA, but not protein levels, depends on a functional 5'–3' decay pathway. (A) *FBA1* mRNA levels when GFP-PP7CP or Dhh1-PP7CP is tethered in *ccr4* Δ , *dcp1* Δ , or *xrn1* Δ strains. (B) Effects of tethered Dhh1-PP7CP on Fba1 protein levels in *ccr4* Δ , *dcp1* Δ , and *xrn1* Δ strains. Tethering assay was performed and analyzed as described in Fig. 1. Mean values \pm SD from three independent experiments are shown.

predicted to lock Dhh1 into the ATP-bound state (Pause and Sonenberg, 1992; Cordin et al., 2006).

A PP7CP-tagged copy of the DQAD mutant protein (Dhh1^{DQAD}-PP7CP) was expressed in *dhh1* Δ cells in which *FBA1* was tagged with a PP7-binding loop. Dhh1^{DQAD}-PP7CP

and wild-type Dhh1-PP7CP were expressed at comparable levels (Fig. S1 B). Intriguingly, Dhh1^{DQAD}-PP7CP reduced both mRNA and protein levels to a similar extent as the wild-type protein when compared with GFP-PP7CP or the non-tethered Dhh1^{DQAD}-GFP control (Fig. 4 A). This demonstrates

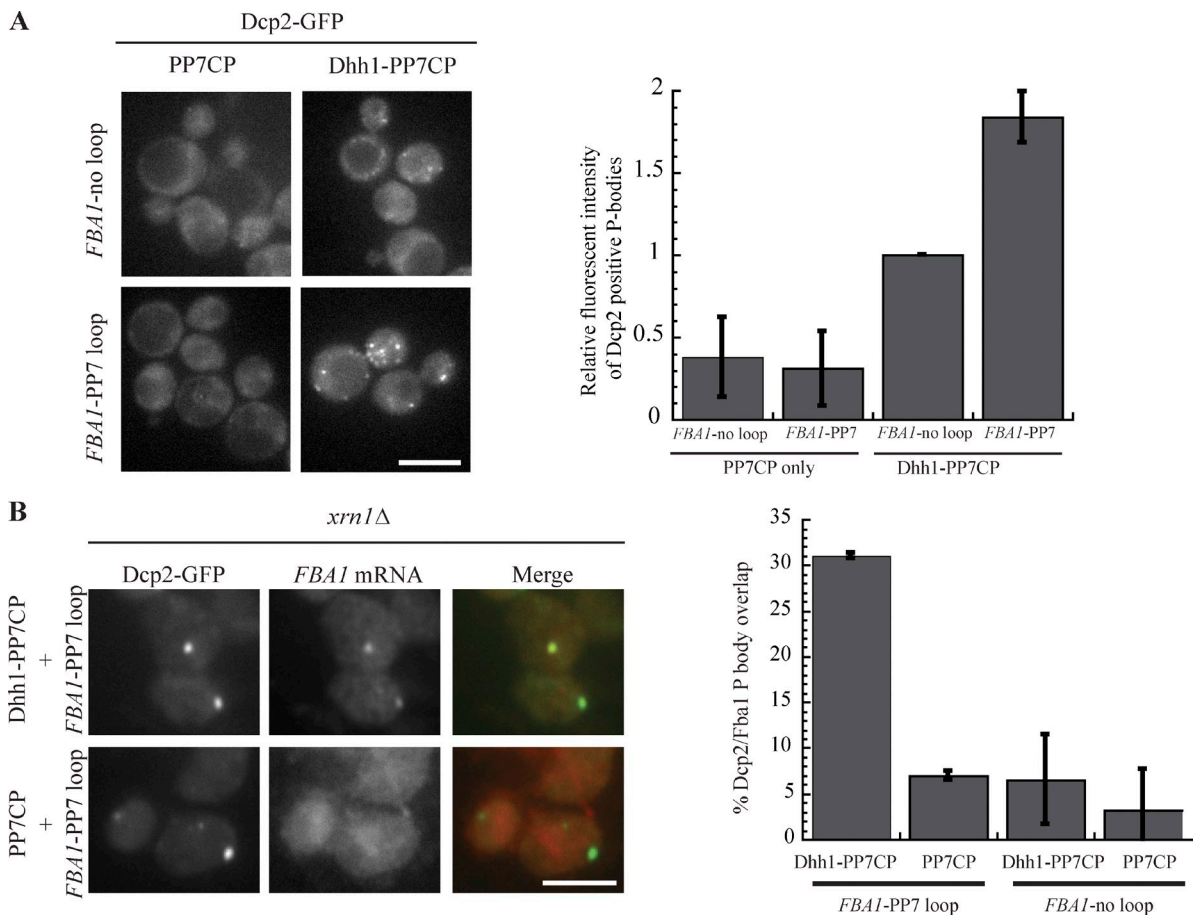


Figure 3. **Tethering Dhh1 to *FBA1* mRNA induces Dcp2-positive PBs and concentrates *FBA1* into PBs.** (A) PBs were visualized with Dcp2-GFP in cells expressing PP7CP or Dhh1-PP7CP proteins and *FBA1* \pm the PP7-binding loop. Fluorescent intensity of Dcp2 PBs was compared with total cell fluorescence for \sim 100 cells. Dcp2 PB fluorescence was normalized to the untethered strain (*FBA1*-no loop) expressing Dhh1-PP7CP, and mean values \pm SD from three independent experiments are shown. (B) PP7CP and Dhh1-PP7CP proteins were expressed in *xrn1Δ* cells with *FBA1* \pm the PP7-binding loop. PBs were visualized with Dcp2-GFP, and *FBA1* mRNA was localized by in situ hybridization. The number of overlapping *FBA1* mRNA/Dcp2 PBs was counted in \sim 150 cells per condition. The graph shows the mean percentage of *FBA1*-containing PBs \pm SD from two independent experiments. Bars, 5 μ m.

that ATP hydrolysis by Dhh1 is not required to reduce RNA and protein levels when Dhh1 is directly targeted to an mRNA.

ATP hydrolysis is necessary for the dynamic localization of Dhh1 in PBs

Although the Dhh1^{DQAD} mutant reduced mRNA and protein levels of tethered mRNAs, expression of Dhh1^{DQAD} was unable to rescue the temperature sensitivity of the *dhh1Δ* strain (Fig. 4 B). Therefore, it was important to further investigate the function of ATP hydrolysis in the cellular role of Dhh1. To address this question, we first tested whether the DQAD mutation affected the interaction with known binding partners of Dhh1. However, no significant difference was seen between the amount of Xrn1-myc or Pat1-myc that copurified with either Dhh1 or Dhh1^{DQAD} in pull-down assays examined by Western blotting (Fig. S2). Furthermore, affinity purifications of Dhh1^{DQAD} revealed that it still interacted with Dcp1, Dcp2, Lsm1, Edc3, and Ccr4 when copurified proteins were analyzed by multidimensional protein identification technology mass spectrometry (unpublished data).

To test whether Dhh1^{DQAD} could function in the decay of nontethered RNAs, we analyzed the decay of three mRNAs,

ACT1, *CGH1*, and *RPL25*, either in cells in which *DHHL* was deleted or in cells expressing wild-type Dhh1 or Dhh1^{DQAD} (Fig. 4 C). All three mRNAs were stabilized in *dhh1Δ* cells compared with wild-type Dhh1-expressing cells (Fig. 4 C). However, the presence of Dhh1^{DQAD} had differential effects on the decay kinetics of the three mRNAs. Whereas Dhh1^{DQAD} fully rescued the defect of *ACT1* decay, it only partially restored the decay of *CRH1* and was not able to rescue *RPL25* decay (Fig. 4 C). Interestingly, the ability of Dhh1^{DQAD} to complement the mRNA turnover defect seemed to correlate with the half-life of the mRNA; Dhh1^{DQAD} fully rescued the decay of the stable *ACT1* mRNA but could not enhance the degradation of the unstable mRNA *RPL25*, suggesting that ATP hydrolysis by Dhh1 may be rate limiting for the decay of short-lived mRNAs. This rate-limiting step may be overcome when Dhh1 is directly tethered to the mRNA.

Next, we monitored the localization of Dhh1-GFP or Dhh1^{DQAD}-GFP in *dhh1Δ* cells. Both proteins were expressed at similar levels (Fig. S1 C). Dhh1-GFP was diffusely localized throughout the cytoplasm in logarithmically growing yeast and localized to PBs only upon stress (Fig. 5 A; Teixeira and Parker, 2007). In contrast, Dhh1^{DQAD}-GFP localized to cytoplasmic foci

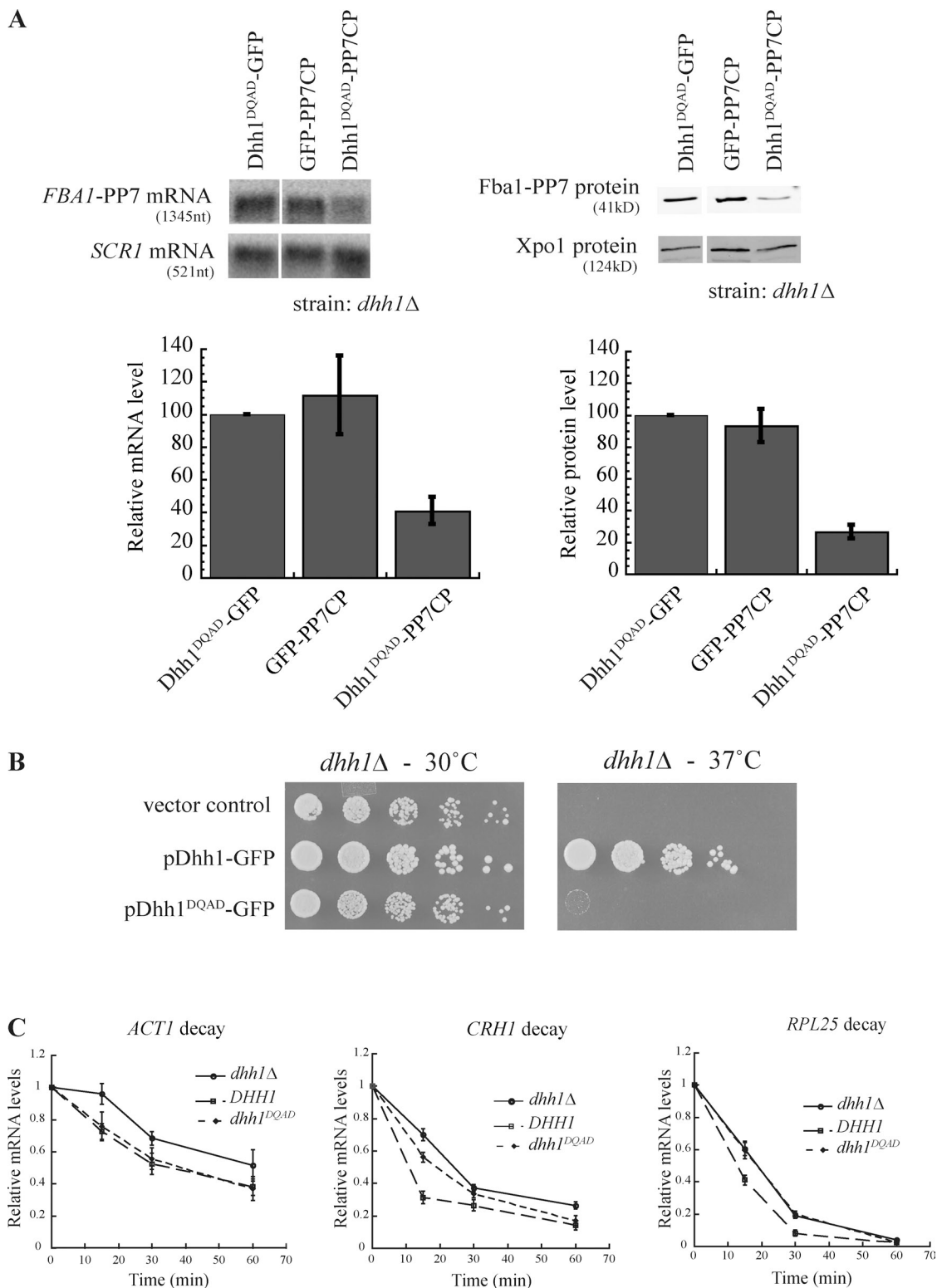


Figure 4. Dhh1^{DQAD} has differential effects on tethered and nontethered mRNAs. (A, left) Northern blot analysis of *FBA1*-PP7 loop mRNA in *dhh1*Δ cells expressing Dhh1^{DQAD}-GFP, GFP-PP7CP, or Dhh1^{DQAD}-PP7CP normalized to *SCR1*. (right) Western blot analysis of *FBA1* protein levels compared with Xpo1. Mean values ± SD from three independent experiments are shown. (B) Wild-type Dhh1 or Dhh1^{DQAD} was expressed in a *dhh1*Δ cells and 10-fold serially diluted. Growth at 30 and 37° was monitored for >3 d. (C) *ACT1*, *CRH1*, and *RPL25* mRNA levels were measured after transcriptional shutoff with thio-lutinin. mRNA decay was observed in *dhh1*Δ cells alone or expressing wild-type Dhh1 or Dhh1^{DQAD}. Graphs depict mean mRNA levels ± SEM from three independent experiments.

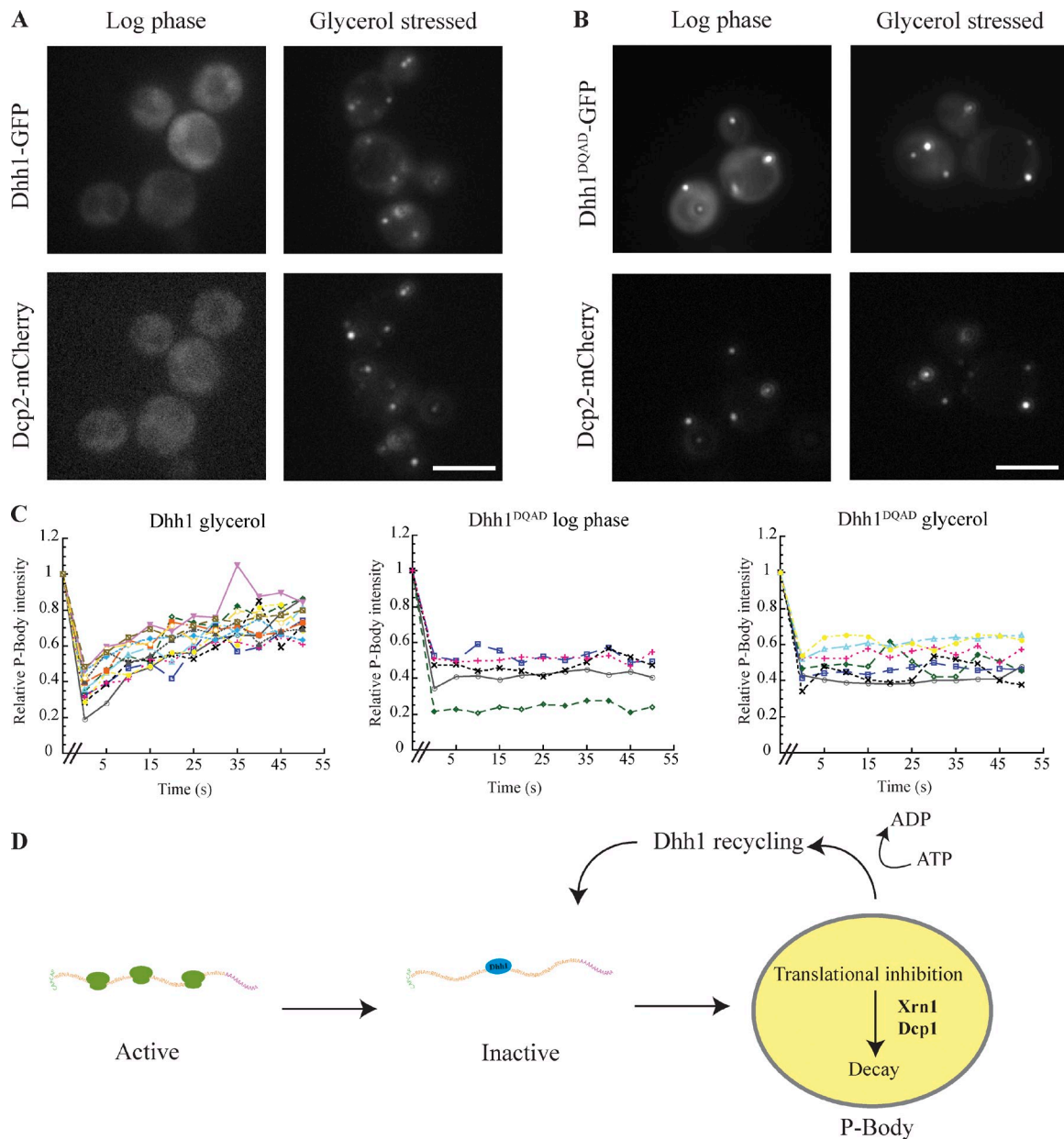


Figure 5. The ATPase function of Dhh1 is required for recycling out of PBs. (A and B) Dhh1-GFP (A) or Dhh1^{DQAD}-GFP (B) proteins were coexpressed with Dcp2-mCherry in *dhh1Δ* cells. Proteins were localized in yeast grown in glucose (A and B, left) or after a shift from glucose to glycerol (A and B, right). Bars, 5 μm. (C) FRAP experiments on Dhh1-GFP and Dhh1^{DQAD}-GFP PBs in yeast growing with glucose or after a glucose to glycerol shift. Representative recovery curves are shown. *n* = 3. (D) A model for Dhh1 function (see Results and discussion for details).

in logarithmically growing cells (Fig. 5 B), and this localization remained unaltered in stress conditions (Fig. 5 B). Dhh1^{DQAD}-GFP and Dcp2-mCherry foci overlapped, suggesting that the Dhh1^{DQAD} foci represent PBs (Fig. 5 B).

Because Dhh1^{DQAD} constitutively localized to PBs, we hypothesized that the ATPase activity of Dhh1 could be critical for the recycling of Dhh1 out of PBs. To test this directly, we performed FRAP experiments (Fig. 5 C). PBs induced upon glycerol stress in the presence of wild-type Dhh1 were dynamic in that the Dhh1-GFP PB signal rapidly recovered (Fig. 5 C, left). This suggests that wild-type Dhh1 continuously cycles in and out of PBs. In contrast, Dhh1^{DQAD}-GFP failed to recover after bleaching PBs in either logarithmically growing or

glycerol-stressed cells (Fig. 5 C, middle and right). No significant recovery could be detected even 1 min after the bleach. Together, these data demonstrate that the Dhh1^{DQAD} protein is trapped in PBs and that ATP hydrolysis by Dhh1 is important for normal PB dynamics.

Our results suggest that ATP hydrolysis is important for the recycling of Dhh1 out of PBs and is required for the decay of certain mRNAs. The mechanism by which ATP hydrolysis stimulates PB disassembly and mRNA turnover remains to be determined. One possibility is that Dhh1 acts as an RNPase facilitating the dissociation of translation factors. Alternatively, although not mutually exclusively, Dhh1 could function as an RNA-dependent scaffold to which decay factors and

translational repressors bind. Such a mode of action would be analogous to the function of the DEXD/H box protein eIF4AIII, which recruits cofactors to the exon junction complex (Ballut et al., 2005; Andersen et al., 2006; Bono et al., 2006). As proposed for eIF4AIII, the ATPase function of Dhh1 could be required for complex disassembly, RNA release, and recycling, consistent with our localization data showing that a hydrolysis-deficient Dhh1 variant constitutively localizes to PBs (Fig. 5). Interestingly, a similar ATPase mutation in the SF1 RNA helicase Upf1, which is involved in NMD, also induces constitutive PBs and prevents mRNP disassembly and completion of NMD (Franks et al., 2010). Collectively, these results suggest that ATP hydrolysis by RNA helicases plays a critical role in enzyme recycling, which is important for the regulation of PB assembly and dynamics.

By tethering Dhh1 to endogenous yeast mRNAs, we directly show that Dhh1 is sufficient to move mRNAs out of active translation into a translationally repressed state in which mRNAs can be targeted for decay (Fig. 5 D). How Dhh1 is recruited to an mRNA in nontethered conditions remains an unresolved question; however, it is probable that recruitment is triggered through the shortening of the poly(A) tail, through interactions with distinct sequence-specific RNA-binding proteins, or in other eukaryotes by miRNA-mediated recruitment of an RNA-induced silencing complex. Our work suggests that recruitment of Dhh1 to mRNAs by miRNAs or other cellular cofactors first triggers translational repression. After the initial step of repression, the mRNA could remain translationally repressed until yet unknown cellular signals direct it to reenter the translational pool, or, alternatively, the recruitment of degradation factors could target the mRNA for decay. The final outcome of whether mRNAs are stored or degraded in response to Dhh1 binding might be highly dependent on cell and tissue type or environmental conditions. Future work will be required to further elucidate the role of Dhh1 in regulating gene expression of specific targets in different cellular conditions and to explore the role of ATP hydrolysis in this process.

Materials and methods

Construction of yeast strains and plasmids

Construction of plasmids for this study (Table S1) was performed using standard molecular cloning techniques. Yeast strains (Table S2) were constructed using PCR-based transformation with specific primers and integration plasmids (Longtine et al., 1998). Additionally, yeast mutants were constructed by transformation with genomic regions PCR amplified from the corresponding yeast mutant strains or by mating and subsequent dissection of the tetrads.

To generate the plasmid used to tag genes with the FLAG tag, the FLAG peptide was cloned into a yeast integration cassette. Plasmids containing the PP7 loop and PP7CP sequences were gifts from B. Hogg and K. Collins (University of California, Berkeley, Berkeley, CA; Hogg and Collins, 2007). The plasmid used for PP7 loop tagging in yeast was a gift from Z. Dossani (University of California, Berkeley). To generate the plasmid used for PP7 loop tagging, the PP7 loop was cloned into a yeast integration plasmid downstream of a FLAG tag. FLAG-PP7-tagged genes were obtained by performing PCR-based plasmid integration. To generate plasmids for expressing proteins tagged with PP7CP, GFP, and CaM-binding peptide (CBP)-tobacco etch virus (TEV)-ZZ, each tag was cloned into a plasmid with the Dhh1 promoter and the Adh1 3' UTR. Protein sequences were then subcloned into these plasmids to generate C-terminal-tagged proteins.

Dhh1 mutagenesis

The Dhh1^{DOGAD} (E196Q) mutation was introduced using a QuikChange site-directed mutagenesis kit (Agilent Technologies) using UC1949 and UC1950 (Table S3) and confirmed by sequencing. This caused a GAA-CAA mutation at base pair 568, which results in an amino acid change from glutamic acid to glutamine.

PP7 tethering assay

Yeast cultures were grown to mid-log phase (OD₆₀₀ 0.4–0.6) at 30°C in synthetic media containing 2% dextrose. Cells were collected by centrifugation and lysed in 1× PBS with Tween 20 using protease inhibitors. Lysis was performed with two 30-s pulses using a Mini-BeadBeater (Biospec Products). Extract was clarified by centrifugation, and extract protein concentration was normalized by Bradford assay (Bio-Rad Laboratories). Protein samples were prepared by resuspending extract in SDS sample buffer. RNA was isolated using the RNeasy RNA isolation kit (QIAGEN).

Northern and Western blot analysis

Total RNA levels were measured using a NanoDrop spectrophotometer (Thermo Fisher Scientific), and equal amounts of total RNA were separated by agarose gel electrophoresis. RNA was transferred to a nitrocellulose membrane and incubated with gene-specific antisense oligonucleotides (Table S3) end labeled with ATP- γ -³²P using T4 polynucleotide kinase (New England Biolabs, Inc.). Hybridization was performed at 46°C in Church buffer; wash steps were performed at 46°C in saline-sodium citrate (SSC) buffer with 0.1% SDS. RNA was visualized using a Typhoon Trio imager (GE Healthcare), and RNA levels were quantified using ImageQuant software (Molecular Dynamics). All tethered mRNAs were monitored by probing with UC587, an oligonucleotide against the FLAG tag. Tethered mRNA levels were normalized against an endogenous untethered mRNA.

Protein samples from yeast extract were separated by SDS-PAGE and used for Western blot analysis with an infrared imaging system (Odyssey; LI-COR Biosciences). Western blotting was performed with one of the following primary antibodies: anti-FLAG, anti-His, anti-myc, anti-Xpo1, or anti-Pab1. Goat anti-mouse Alexa Fluor 680 (Invitrogen) or goat anti-rabbit IRDye800 (Rockland Immunochemicals) was used as a secondary antibody. Protein levels were quantified using the Odyssey imaging software. Protein levels of tethered mRNAs were monitored by probing an antibody against the FLAG tag. Protein levels were normalized against the endogenous Xpo1 or Pab1 protein.

mRNA decay measurements

Cell cultures were grown to log phase. Time points were collected after the addition of 3 μ g/ml thiolutin (Enzo Life Sciences). RNA isolation was performed as described in the PP7 tethering assay section. After DNase treatment (Invitrogen) of the RNA, cDNA was synthesized with reverse transcription (SuperScript II; Invitrogen). Quantitative PCR was performed in a real-time PCR system (StepOnePlus; Applied Biosystems) using gene-specific primers and green ROX mix (Absolute QPCR SYBR; Thermo Fisher Scientific). cDNA levels were normalized against levels of the RNA subunit of the signal recognition particle SCR1.

Myc purifications

Purifications were performed as described in Oeffinger et al. (2007). In brief, cells were grown to mid-log phase and lysed mechanically using a mixer mill (type 307; Retsch). Grindate was resuspended in TBT buffer (20 mM Hepes, pH 7.4, 110 mM KOAc, 2 mM MgCl₂, 0.5% Triton X-100, 0.1% Tween 20, 1:1,000 DTT, 1:5,000 rNasin [Promega], and 1:5,000 Antifoam B [Sigma-Aldrich]), and extract was incubated with IgG-coupled magnetic Dynabeads (Invitrogen). Beads were washed twice in TBT buffer and resuspended in SDS sample buffer.

Live-cell fluorescent microscopy

Cells were grown to mid-log phase (OD₆₀₀ 0.4–0.6) at 30°C in synthetic media containing 2% dextrose. Cells were observed using a fluorescence microscope (Eclipse E600; Nikon) using a 100× oil immersion objective. Images were captured using a charge-coupled device camera (Orca II, C4742-98-24R; Hamamatsu Photonics) controlled by MetaMorph software (4.6R6; Molecular Devices).

For tethering experiments measuring the accumulation of Dcp2-GFP in PBs, the fluorescent intensity of Dcp2 in PBs was compared with the fluorescent intensity of the entire cell for ~100 cells per indicated condition. The amount of Dcp2 in PBs was then normalized to the untethered strain expressing Dhh1-PP7CP for each independent replicate. Quantification was

performed using ImageJ, a public domain Java image-processing program (National Institutes of Health).

For carbon source shift experiments, cells were washed twice in fresh synthetic media containing either 2% dextrose or 3% glycerol as a carbon source. Cells were resuspended in the same medium used for washing and observed after 15 min. Image processing was performed using Photoshop (Adobe).

In situ hybridizations

Four oligonucleotides were designed against regions of *FBA1* mRNA (Table S3) and used to create fluorescently labeled RNA probes. The protocol for in vitro transcription and fluorescent labeling was based on manufacturer's instructions and published protocols from Robert Singer's laboratory (Long et al., 1995). RNA probes were synthesized by in vitro transcription using reagents from the MEGAshortscript kit (Applied Biosystems). RNA probes were synthesized by a standard in vitro transcription reaction, except that UTP was replaced by a 1:1 mixture of UTP/aminallyl UTP. Transcription reactions were then treated with DNase, phenol extracted, ethanol precipitated, and resuspended in 1× SSC. Unincorporated nucleotides were removed by gel filtration through spin columns (NucAway; Invitrogen). The probes were then ethanol precipitated and resuspended in 0.1 M NaHCO₃ buffer, pH 8.8. The four *FBA1* probes were combined into one reaction (1.5 µg of each probe) and labeled using one vial of the Cy3 monoreactive labeling kit (GE Healthcare). Unincorporated nucleotides were removed by two rounds of ethanol precipitation and were resuspended in water.

Cultures were grown to mid-log phase (OD₆₀₀ 0.4–0.6) at 30°C in synthetic media with 2% dextrose. 1 ml of cell culture was fixed for 15 min with 134 µl of 37% formaldehyde (Flukka) and washed twice in buffer A (0.01 M potassium phosphate buffer, pH 6.5, and 0.5 mM MgCl₂) followed by resuspension in buffer B (0.01 M potassium phosphate buffer, pH 6.5, 0.5 mM MgCl₂, and 1.2 M sorbitol). Cells were spheroplasted with zymolase T100, plated on poly-L-lysine-coated slides, and incubated in 70% ethanol for 2 h. Samples were then blocked for 30 min at 37° in hybridization buffer and incubated overnight with Cy3-labeled RNA probes against *FBA1* mRNA. Slides were washed with decreasing concentrations of SSC and mounted in Vectashield mounting medium (Vector Laboratories). *FBA1* mRNA was colocalized with Dcp2-GFP, and the number of overlapping *FBA1* and Dcp2 PBs was counted in ~150 cells per condition.

FRAP

Photobleaching was performed using a DeltaVision microscope (Spectris; Applied Precision) equipped with a 488-nm DeltaVision quantifiable laser module (Applied Precision) and a camera (CoolSnap HQ; Photometrics). One z stack image (with optical sections 0.5 µm apart) was collected before photobleaching. PBs to be photobleached were subjected to a 1–2-s pulse from a UV laser. Images were collected at 5-s intervals for 1 min after bleach. Images were deconvolved using softWoRx software (Applied Precision), and a maximum projection from each z stack was obtained using softWoRx image-processing software. Data analysis was performed using ImageJ.

Online supplemental material

Fig. S1 shows that PP7CP and GFP fusion proteins are expressed to similar levels and that the Dhh1-PP7CP-induced reduction of *FBA1* mRNA and protein levels is specific to tethered Dhh1. In Fig. S2, we demonstrate that equal amounts of mRNA decay factors copurify with wild-type and ATPase mutant Dhh1. Tables S1–S3 describe yeast strains (Table S1), plasmids (Table S2), and oligonucleotides (Table S3) used in this study. Online supplemental material is available at <http://www.jcb.org/cgi/content/full/jcb.201007151/DC1>.

We are grateful to Zain Dossani and Chris Mugler for technical and experimental help. We would also like to thank Serafin Colmenares for his assistance with FRAP studies, Sebastien Huet and Jan Ellenberg for initial help with the FRAP experiments, and Lori Kohlstaedt for the mass spectrometry analysis. We would also like to acknowledge Kathy Collins and Bobby Hogg for giving us plasmids containing the PP7 loop and PP7CP sequences and Jeremy Thorne for providing us with the mCherry integration plasmid. We would like to thank Leon Chan, Zain Dossani, Ben Montipetit, and other members of the Weis laboratory for helpful discussions and comments on the manuscript.

This work was supported by grants from the National Institutes of Health to K. Weis (RC1GM91533 and RO1GM58065).

Submitted: 27 July 2010

Accepted: 21 July 2011

References

- Andersen, C.B., L. Ballut, J.S. Johansen, H. Chamieh, K.H. Nielsen, C.L. Oliveira, J.S. Pedersen, B. Séraphin, H. Le Hir, and G.R. Andersen. 2006. Structure of the exon junction core complex with a trapped DEAD-box ATPase bound to RNA. *Science*. 313:1968–1972. doi:10.1126/science.1131981
- Anderson, P., and N. Kedersha. 2006. RNA granules. *J. Cell Biol.* 172:803–808. doi:10.1083/jcb.200512082
- Ballut, L., B. Marchadier, A. Bague, C. Tomasetto, B. Séraphin, and H. Le Hir. 2005. The exon junction core complex is locked onto RNA by inhibition of eIF4AIII ATPase activity. *Nat. Struct. Mol. Biol.* 12:861–869. doi:10.1038/nsmb990
- Boag, P.R., A. Atalay, S. Robida, V. Reinke, and T.K. Blackwell. 2008. Protection of specific maternal messenger RNAs by the P body protein CGH-1 (Dhh1/RCK) during *Caenorhabditis elegans* oogenesis. *J. Cell Biol.* 182:543–557. doi:10.1083/jcb.200801183
- Bono, F., J. Ebert, E. Lorentzen, and E. Conti. 2006. The crystal structure of the exon junction complex reveals how it maintains a stable grip on mRNA. *Cell*. 126:713–725. doi:10.1016/j.cell.2006.08.006
- Chu, C.Y., and T.M. Rana. 2006. Translation repression in human cells by microRNA-induced gene silencing requires RCK/p54. *PLoS Biol.* 4:e210. doi:10.1371/journal.pbio.0040210
- Coller, J., and R. Parker. 2004. Eukaryotic mRNA decapping. *Annu. Rev. Biochem.* 73:861–890. doi:10.1146/annurev.biochem.73.011303.074032
- Coller, J., and R. Parker. 2005. General translational repression by activators of mRNA decapping. *Cell*. 122:875–886. doi:10.1016/j.cell.2005.07.012
- Coller, J.M., M. Tucker, U. Sheth, M.A. Valencia-Sanchez, and R. Parker. 2001. The DEAD box helicase, Dhh1p, functions in mRNA decapping and interacts with both the decapping and deadenylase complexes. *RNA*. 7:1717–1727. doi:10.1017/S135583820101994X
- Cordin, O., J. Banroques, N.K. Tanner, and P. Linder. 2006. The DEAD-box protein family of RNA helicases. *Gene*. 367:17–37. doi:10.1016/j.gene.2005.10.019
- Curtis, D., R. Lehmann, and P.D. Zamore. 1995. Translational regulation in development. *Cell*. 81:171–178. doi:10.1016/0092-8674(95)90325-9
- Eulalio, A., I. Behm-Ansmant, and E. Izaurralde. 2007. P bodies: at the crossroads of post-transcriptional pathways. *Nat. Rev. Mol. Cell Biol.* 8:9–22. doi:10.1038/nrm2080
- Fischer, N., and K. Weis. 2002. The DEAD box protein Dhh1 stimulates the decapping enzyme Dcp1. *EMBO J.* 21:2788–2797. doi:10.1093/emboj/21.11.2788
- Franks, T.M., and J. Lykke-Andersen. 2008. The control of mRNA decapping and P-body formation. *Mol. Cell*. 32:605–615. doi:10.1016/j.molcel.2008.11.001
- Franks, T.M., G. Singh, and J. Lykke-Andersen. 2010. Upf1 ATPase-dependent mRNP disassembly is required for completion of nonsense-mediated mRNA decay. *Cell*. 143:938–950. doi:10.1016/j.cell.2010.11.043
- Garneau, N.L., J. Wilusz, and C.J. Wilusz. 2007. The highways and byways of mRNA decay. *Nat. Rev. Mol. Cell Biol.* 8:113–126. doi:10.1038/nrm2104
- Gillian-Daniel, D.L., N.K. Gray, J. Åström, A. Barkoff, and M. Wickens. 1998. Modifications of the 5' cap of mRNAs during *Xenopus* oocyte maturation: independence from changes in poly(A) length and impact on translation. *Mol. Cell Biol.* 18:6152–6163.
- Hogg, J.R., and K. Collins. 2007. RNA-based affinity purification reveals 7SK RNPs with distinct composition and regulation. *RNA*. 13:868–880. doi:10.1261/ma.565207
- Holstege, F.C., E.G. Jennings, J.J. Wyrick, T.I. Lee, C.J. Hengartner, M.R. Green, T.R. Golub, E.S. Lander, and R.A. Young. 1998. Dissecting the regulatory circuitry of a eukaryotic genome. *Cell*. 95:717–728. doi:10.1016/S0092-8674(00)81641-4
- Long, R.M., D.J. Elliott, F. Stutz, M. Rosbash, and R.H. Singer. 1995. Spatial consequences of defective processing of specific yeast mRNAs revealed by fluorescent in situ hybridization. *RNA*. 1:1071–1078.
- Longtine, M.S., A. McKenzie III, D.J. Demarini, N.G. Shah, A. Wach, A. Brachat, P. Philippsen, and J.R. Pringle. 1998. Additional modules for versatile and economical PCR-based gene deletion and modification in *Saccharomyces cerevisiae*. *Yeast*. 14:953–961. doi:10.1002/(SICI)1097-0061(199807)14:10<953::AID-YEA293>3.0.CO;2-U
- Maekawa, H., T. Nakagawa, Y. Uno, K. Kitamura, and C. Shimoda. 1994. The ste13+ gene encoding a putative RNA helicase is essential for nitrogen starvation-induced G1 arrest and initiation of sexual development in the fission yeast *Schizosaccharomyces pombe*. *Mol. Gen. Genet.* 244:456–464. doi:10.1007/BF00583896
- Maillet, L., and M.A. Collart. 2002. Interaction between Not1p, a component of the Ccr4-not complex, a global regulator of transcription, and Dhh1p, a

- putative RNA helicase. *J. Biol. Chem.* 277:2835–2842. doi:10.1074/jbc.M107979200
- Minshall, N., and N. Standart. 2004. The active form of Xp54 RNA helicase in translational repression is an RNA-mediated oligomer. *Nucleic Acids Res.* 32:1325–1334. doi:10.1093/nar/gkh303
- Minshall, N., G. Thom, and N. Standart. 2001. A conserved role of a DEAD box helicase in mRNA masking. *RNA.* 7:1728–1742. doi:10.1017/S135583820101158X
- Minshall, N., M. Kress, D. Weil, and N. Standart. 2009. Role of p54 RNA helicase activity and its C-terminal domain in translational repression, P-body localization and assembly. *Mol. Biol. Cell.* 20:2464–2472. doi:10.1091/mbc.E09-01-0035
- Nakamura, A., R. Amikura, K. Hanyu, and S. Kobayashi. 2001. Me31B silences translation of oocyte-localizing RNAs through the formation of cytoplasmic RNP complex during *Drosophila* oogenesis. *Development.* 128:3233–3242.
- Navarro, R.E., E.Y. Shim, Y. Kohara, A. Singson, and T.K. Blackwell. 2001. cgh-1, a conserved predicted RNA helicase required for gametogenesis and protection from physiological germline apoptosis in *C. elegans*. *Development.* 128:3221–3232.
- Oeffinger, M., K.E. Wei, R. Rogers, J.A. DeGrasse, B.T. Chait, J.D. Aitchison, and M.P. Rout. 2007. Comprehensive analysis of diverse ribonucleoprotein complexes. *Nat. Methods.* 4:951–956. doi:10.1038/nmeth1101
- Parker, R., and U. Sheth. 2007. P bodies and the control of mRNA translation and degradation. *Mol. Cell.* 25:635–646. doi:10.1016/j.molcel.2007.02.011
- Pause, A., and N. Sonenberg. 1992. Mutational analysis of a DEAD box RNA helicase: the mammalian translation initiation factor eIF-4A. *EMBO J.* 11:2643–2654.
- Rocak, S., and P. Linder. 2004. DEAD-box proteins: the driving forces behind RNA metabolism. *Nat. Rev. Mol. Cell Biol.* 5:232–241. doi:10.1038/nrm1335
- Sheth, U., and R. Parker. 2003. Decapping and decay of messenger RNA occur in cytoplasmic processing bodies. *Science.* 300:805–808. doi:10.1126/science.1082320
- Talarek, N., E. Cameroni, M. Jaquenoud, X. Luo, S. Bontron, S. Lippman, G. Devgan, M. Snyder, J.R. Broach, and C. De Virgilio. 2010. Initiation of the TORC1-regulated G0 program requires Igo1/2, which license specific mRNAs to evade degradation via the 5'-3' mRNA decay pathway. *Mol. Cell.* 38:345–355. doi:10.1016/j.molcel.2010.02.039
- Teixeira, D., and R. Parker. 2007. Analysis of P-body assembly in *Saccharomyces cerevisiae*. *Mol. Biol. Cell.* 18:2274–2287. doi:10.1091/mbc.E07-03-0199
- Teixeira, D., U. Sheth, M.A. Valencia-Sanchez, M. Brengues, and R. Parker. 2005. Processing bodies require RNA for assembly and contain nontranslating mRNAs. *RNA.* 11:371–382. doi:10.1261/rna.7258505
- Tritschler, F., J.E. Braun, A. Eulalio, V. Truffault, E. Izaurralde, and O. Weichenrieder. 2009. Structural basis for the mutually exclusive anchoring of P body components EDC3 and Tral to the DEAD box protein DDX6/Me31B. *Mol. Cell.* 33:661–668. doi:10.1016/j.molcel.2009.02.014
- Tseng-Rogenski, S.S., J.L. Chong, C.B. Thomas, S. Enomoto, J. Berman, and T.H. Chang. 2003. Functional conservation of Dhh1p, a cytoplasmic DExD/H-box protein present in large complexes. *Nucleic Acids Res.* 31:4995–5002. doi:10.1093/nar/gkg712
- Tucker, M., M.A. Valencia-Sanchez, R.R. Staples, J. Chen, C.L. Denis, and R. Parker. 2001. The transcription factor associated Ccr4 and Caf1 proteins are components of the major cytoplasmic mRNA deadenylase in *Saccharomyces cerevisiae*. *Cell.* 104:377–386. doi:10.1016/S0092-8674(01)00225-2
- Westmoreland, T.J., J.A. Olson, W.Y. Saito, G. Huper, J.R. Marks, and C.B. Bennett. 2003. Dhh1 regulates the G1/S-checkpoint following DNA damage or BRCA1 expression in yeast. *J. Surg. Res.* 113:62–73. doi:10.1016/S0022-4804(03)00155-0
- Weston, A., and J. Sommerville. 2006. Xp54 and related (DDX6-like) RNA helicases: roles in messenger RNP assembly, translation regulation and RNA degradation. *Nucleic Acids Res.* 34:3082–3094. doi:10.1093/nar/gkl409